JOURNAL OF SOLID STATE CHEMISTRY 26, 345–355 (1978)

The Crystal Structure of $Ba_2V_2O_7$

F. C. HAWTHORNE

Department of Earth Sciences, University of Manitoba, Winnipeg, Manitoba, Canada, R3T 2N2

AND C. CALVO

Department of Chemistry, McMaster University, Hamilton, Ontario, Canada, L8S 4M1

Received February 21, 1978; in revised form May 11, 1978

$Ba_2V_2O_7$ is triclinic with $a = 13.571(3)$, $b = 7.320(2)$, $c = 7.306(2)$ Å, $\alpha = 90.09(1)$, $\beta = 99.48(1)$, $\gamma = 87.32(1)°$, $V = 715.1$ Å^3, $Z = 4$, and space group $P\bar{1}$. The crystal structure was solved by Patterson and Fourier methods and refined by full-matrix least-squares analysis to a R_w of 0.034 ($R = 0.034$) using 2484 reflections measured on a Syntex $P\bar{1}$ automatic four-circle diffractometer. The structure has two unique divanadate groups that are repeated by the b and c lattice translations to form sheets of divanadate groups parallel to (100). These sheets are linked by four unique Ba atoms that lie between these sheets. Ba(1) and Ba(3) are coordinated by eight oxygens arranged in a distorted biaugmented triangular prism and a distorted cubic antiprism, respectively. Ba(2) is coordinated by 10 oxygens arranged in a distorted gyro-elongated square dipyramid and Ba(4) is coordinated by nine oxygens arranged in a distorted tri-augmented triangular prism. These coordination numbers are substantiated by a bond strength analysis of the structure, and the variation in ⟨Ba–O⟩ distances is compatible with the assigned cation and anion coordination numbers. Both divanadate groups are in the eclipsed configuraton with ⟨V–O(br)⟩ bond lengths of 1.821(4) and 1.824(4) Å and V–O(br)–V angles of 125.6(3) and 123.7(3)°, respectively. Examination of the divanadate groups in a series of structures allows certain generalizations to be made. Longer ⟨V–O(br)⟩ bond lengths are generally associated with smaller V–O(br)–V angles. When V–O(br)–V < 140°, the divanadate group is generally in an eclipsed configuration; when V–O(br)–V > 140°, the divanadate group is generally in a staggered configuration. Nontetrahedral cations with large coordination numbers require more oxygens with which to bond, and hence O(br) is more likely to be three coordinate, with the divanadate group in the eclipsed configuration. In the eclipsed configuration, decrease in V–O(br)–V promotes bonding between O(br) and nontetrahedral cations, and hence smaller nontetrahedral cations are generally associated with smaller V–O–(br)–V angles.

Introduction

Crystals with the general stoichiometry $M_2T_2O_7$ show a wide variety of structure types. Where the ionic radius (*1*) of the T cation is greater than ~0.5 Å, the coordination number of the T cation is [6], and the resulting structures are related to that of atopite. When the ionic radius of the T cation is less than 0.5 Å, the coordination number of the T cation is [4] and the structures are characterized by isolated pairs of corner-sharing tetrahedra of the form $(T_2^{n+}O_7^{2-})^{-2(7-n)}$. Brown and Calvo (*3*) showed that when the ionic radius of the M cation is less than ~0.97 Å, the structures are generally related to that of thortveitite whereas

0022-4596/78/0264-0345$02.00/0
Copyright © 1978 by Academic Press, Inc.
All rights of reproduction in any form reserved.
Printed in Great Britain

when the ionic radius of the M cation is greater than ~0.97 Å, the structures are of the dichromate type. Baglio and Dann (*2*) further showed that the M cation radius at which the boundary between the thortveitite and dichromate structures occurred is a function of the T cation radius. In the thortveitite structure, the tetrahedral pair occurs in a staggered configuration whereas in the dichromate structures, this unit is in the eclipsed configuration. In addition, the thorveitite structures are characterized by [5]- and [6]-fold coordination of the M cations whereas the dichromate structures are characterized by M cation coordination numbers from [7] to [10].

Recent work on the structures of $Co_2V_2O_7$ and $Ni_2V_2O_7$ (*4*) showed that these compounds possess an eclipsed $(V_2^{5+}O_7)^{3-}$ configuration, and are more related to the dichromate structures than to the thortveitite-type structures. These results are at odds with the simple model for the $M_2T_2O_7$ structures outlined above, and prompted this examination of the $M_2^{2+}V_2O_7$ structure. It is perhaps notable that the above model failed for Ni and Co, some of the smallest M-type cations in this series. In order to extend the data to large M-type cation values, we examine here the structure of $Ba_2V_2O_7$. Kohlmuller and Perraud (*5*) synthesized $Ba_2V_2O_7$ and indicated that it is dimorphic. Fortiev *et al.* (*6*) suggested that one of the "phases" was actually a mixture. However, on the basis of optics they indicated that $Ba_2V_2O_7$ is monoclinic whereas the crystals examined during the present study were triclinic. Thus the possibility of polymorphism in $Ba_2V_2O_7$ cannot be discounted.

Experimental

Crystals of $Ba_2V_2O_7$ were prepared by heating stoichiometric amounts of BaO and V_2O_5 in a platinum crucible. The mixture was held at 1100°C for 24 hr, cooled to 600°C at 6°C/hr, and then quenched to room temperature. Precession photographs exhibited triclinic symmetry, and a primitive cell was chosen. Cell dimensions were determined by least-squares refinement of 15 reflections automatically aligned on a 4-circle diffractometer; the following values were obtained: a = 13.571(3), b = 7.320(2), c = 7.306(2) Å, α = 90.09(1), β = 99.48(1), γ = 87.32(1)°, V = 715.1 Å^3.

The crystal used in the collection of the intensity data was an irregular equidimensional fragment ~0.08 mm in diameter. The crystal was mounted on a Syntex $P\bar{1}$ automatic diffractometer using graphite-monochromated Mo$K\alpha$ radiation (λ = 0.71069 Å) and a scintillation counter. Intensities were collected in the $\theta = 2\theta$ scan mode at variable rates from 2.0 to 24.0°/min., depending on the peak count through an angle of 2° and the α_1–α_2 separation. Background counts were made at the beginning and end of each scan. A standard reflection was examined every 50 reflections to check on the crystal alignment; no significant variation was noted throughout the data collection. Reflections were collected over one asymmetric unit out to a 2θ value of 60°. Intensities were corrected for absorption (μR = 1.11), Lorentz, polarization and background effects and reduced to structure factors, using the X-ray 67 Program System for X-ray Crystallography (*7*). A reflection was considered as observed if its magnitude exceeded that of three standard deviations based on counting statistics; this resulted in 2822 reflections of which 2484 were considered as observed.

The positions of the four distinct Ba atoms were derived from a three-dimensional Patterson map and subsequent least-squares refinement led to a R_w of 0.34 where

$$R_w = \left[\frac{\sum w(|F_o| - |F_c|)^2}{\sum w|F_o|^2} \right]^{1/2}.$$

A difference-Fourier map revealed 4 vanadium and 12 oxygen positions and refinement of all positional parameters converged at $R_w = 0.09$. A subsequent difference-Fourier map revealed the remaining oxygen positions and further

TABLE II

ATOMIC AND THERMAL PARAMETERS FOR $Ba_2V_2O_7$

	x	y	z	U_{11}[b]	U_{22}	U_{33}	U_{12}	U_{13}	U_{23}
Ba(1)	0.64150(4)	0.85756(6)	0.12758(6)	78(3)	108(2)	122(2)	5(2)	20(2)	6(2)
Ba(2)	0.65492(4)	0.27374(6)	0.74429(6)	96(3)	93(2)	126(2)	15(2)	57(2)	2(2)
Ba(3)	0.14088(4)	0.16666(6)	0.28502(6)	77(3)	116(2)	99(2)	16(2)	15(2)	−37(2)
Ba(4)	0.15766(4)	0.58576(6)	0.66859(6)	81(3)	98(2)	73(2)	14(2)	12(2)	−2(2)
V(1)	0.3960(1)	0.2681(2)	0.4022(2)	63(7)	98(6)	71(5)	0(5)	13(5)	−11(4)
V(2)	0.5864(1)	0.3265(2)	0.1969(2)	71(7)	85(5)	72(5)	0(5)	23(5)	−14(4)
V(3)	0.1068(1)	0.0659(2)	0.8033(2)	62(7)	86(6)	67(5)	11(5)	11(5)	−9(4)
V(4)	0.9169(1)	0.3439(2)	0.8110(2)	56(7)	89(5)	62(5)	14(5)	18(5)	−15(4)
O(1)	0.8022(4)	0.0264(7)	0.0355(7)	69(31)	164(27)	132(25)	49(22)	10(22)	40(20)
O(2)	0.6519(4)	0.4910(7)	0.1176(7)	127(33)	146(26)	153(26)	−58(22)	46(23)	−3(21)
O(3)	0.3454(4)	0.1013(7)	0.2613(7)	194(35)	136(26)	119(25)	25(23)	3(23)	−45(20)
O(4)	0.4744(4)	0.4080(7)	0.2858(8)	130(32)	95(25)	193(27)	42(22)	90(24)	13(21)
O(5)	0.0449(4)	0.4932(7)	0.3233(7)	119(32)	110(25)	93(24)	−8(21)	37(21)	−4(19)
O(6)	0.9518(4)	0.1008(7)	0.3194(8)	134(33)	133(26)	163(27)	5(22)	29(23)	−61(21)
O(7)	0.1585(4)	0.7893(7)	0.3367(7)	130(32)	135(26)	106(25)	−10(22)	30(22)	−30(20)
O(8)	0.6641(4)	0.2033(7)	0.3552(7)	155(34)	138(26)	135(26)	20(23)	11(23)	11(21)
O(9)	0.5381(4)	0.8178(8)	0.4023(7)	118(33)	217(29)	130(26)	6(24)	19(23)	12(22)
O(10)	0.2990(4)	0.4047(8)	0.4450(8)	147(34)	155(28)	215(28)	−3(24)	89(25)	−48(22)
O(11)	0.5523(4)	0.1828(7)	0.0160(7)	113(31)	101(25)	118(25)	−3(22)	14(22)	−50(19)
O(12)	0.1528(5)	0.5524(8)	0.0479(7)	188(25)	224(30)	107(27)	58(25)	100(24)	−46(22)
O(13)	0.9769(4)	0.8000(7)	0.0735(7)	74(32)	145(26)	156(26)	69(22)	21(22)	−17(21)
O(14)	0.8351(4)	0.7980(7)	0.3299(7)	133(32)	130(26)	132(26)	4(22)	12(23)	16(20)

[a] Calculated from $\beta_{ij} = 2\pi^2 b_i b_j U_{ij}$ where b_i and b_j are the reciprocal lattice vectors and $U_{ij} = U_{ij} \times 10^4$.

refinement converged to an $R_w = 0.052$ with individual isotropic temperature factors. A Cruickshank weighting scheme was used in which $w = (6.31–0.0297\ |F_0| + 0.00042|F_0|^2)$, where the weights w were chosen so as to make $w(|F_0| - |F_c|)^2$ independent of the variation in $|F_0|$. Further refinement using anisotropic temperature factors for all atoms resulted in convergence at an R of 0.034 and an R_w of 0.034. Scattering factors for neutral atoms were taken from Cromer and Mann (*8*) with anomalous dispersion terms from Cromer and Liberman (*9*). Table I[1] lists the observed and calculated structure factors and Table II gives the atomic coordinates and anisotropic temperature factors. Interatomic distances and angles are listed in Tables III to V.

[1] Table I has been deposited as Document No. NAPS 03280 with the National Auxiliary Publications Service, c/o Microfiche Publications, 440 Park Avenue South, New York, New York 10006. A copy may be secured by citing the document number and by remitting $5.00 for photocopy or $1.50 for microfiche. Advance payment is required. Make cheque or money order payable to Microfiche Publications.

Discussion

The structure of $Ba_2V_2O_7$ is shown in Fig. 1. The four unique V atoms are tetrahedrally coordinated, and adjacent tetrahedra share one vertex to form two distinct divanadate groups, both of which are approximately in the eclipsed configuration. Each of the divanadate groups is repeated by a center of symmetry and the *b* and *c* lattice translations to form two sheets (*3*) that are approximately perpendicular to the *a*-axis (see Fig. 2). These sheets are linked together to Ba atoms; the overall arrangement is isostructural with $K_2Cr_2O_7$ (*23*, *24*).

It is often difficult to assign an unambiguous

TABLE III

BOND LENGTHS IN $Ba_2V_2O_7$

V(1)–O(3)	1.692(6) Å	V(2)–O(2)	1.688(6) Å
V(1)–O(4)	1.818(6)	V(2)–O(4)	1.823(6)
V(1)–O(9)	1.663(5)	V(2)–O(8)	1.666(5)
V(1)–O(10)	1.687(6)	V(2)–O(11)	1.705(5)
⟨V(1)–O⟩	1.715	⟨V(2)–O⟩	1.721
V(3)–O(1)	1.677(5)	V(4)–O(5)	1.697(5)
V(3)–O(6)	1.666(6)	V(4)–O(7)	1.699(5)
V(3)–O(13)	1.815(6)	V(4)–O(12)	1.669(6)
V(3)–O(14)	1.701(6)	V(4)–O(13)	1.832(5)
⟨V(3)–O⟩	1.715	⟨V(4)–O⟩	1.724
Ba(1)–O(1)	2.734(6)	Ba(3)–O(1)	2.926(6)
Ba(1)–O(2)	2.682(5)	Ba(3)–O(3)	2.828(6)
Ba(1)–O(3)	2.893(6)	Ba(3)–O(5)	2.705(5)
Ba(1)–O(8)	3.026(5)	Ba(3)–O(6)	2.684(6)
Ba(1)–O(9)	2.655(6)	Ba(3)–O(7)	2.782(5)
Ba(1)–O(11)	2.685(5)	Ba(3)–O(10)	2.919(6)
Ba(1)–O(11)	2.696(5)	Ba(3)–O(13)	2.840(5)
Ba(1)–O(14)	2.809(5)	Ba(3)–O(14)	2.791(5)
⟨Ba(1)–O⟩	2.773	⟨Ba(3)–O⟩	2.809
Ba(2)–O(1)	3.174(5)	Ba(4)–O(2)	2.823(5)
Ba(2)–O(2)	3.160(6)	Ba(4)–O(5)	2.826(5)
Ba(2)–O(3)	2.746(5)	Ba(4)–O(5)	2.845(6)
Ba(2)–O(4)	2.837(5)	Ba(4)–O(6)	2.684(5)
Ba(2)–O(7)	2.713(6)	Ba(4)–O(7)	2.850(5)
Ba(2)–O(8)	2.911(5)	Ba(4)–O(8)	2.959(6)
Ba(2)–O(9)	2.774(6)	Ba(4)–O(10)	2.982(6)
Ba(2)–O(10)	2.877(6)	Ba(4)–O(12)	2.794(5)
Ba(2)–O(11)	2.706(6)	Ba(4)–O(14)	2.806(5)
Ba(2)–O(12)	3.120(6)	⟨Ba(4)–O⟩	2.841
⟨Ba(2)–O⟩	2.902		

TABLE IV

POLYHEDRON EDGE LENGTHS IN $Ba_2V_2O_7$

V(1) Tetrahedron		V(2) Tetrahedron	
O(3)–O(4)	2.898(8) Å	O(2)–O(4)	2.966(9) Å
O(3)–O(9)	2.774(7)	O(2)–O(8)	2.713(8)[a]
O(3)–O(10)	2.696(8)[a]	O(2)–O(11)	2.724(8)
O(4)–O(9)	2.850(8)	O(4)–O(8)	2.888(8)[a]
O(4)–O(10)	2.818(9)[a]	O(4)–O(11)	2.869(8)
O(9)–O(10)	2.765(8)	O(8)–O(11)	2.692(7)[a]
⟨O–O⟩	2.800	⟨O–O⟩	2.809
V(3) Tetrahedron		V(4) Tetrahedron	
O(1)–O(6)	2.726(7)	O(5)–O(7)	2.710(8)[a]
O(1)–O(13)	2.804(8)[a]	O(5)–O(12)	2.723(8)
O(1)–O(14)	2.693(7)[a]	O(5)–O(13)	2.914(7)
O(6)–O(13)	2.882(8)	O(7)–O(12)	2.722(8)[a]
O(6)–O(14)	2.793(8)	O(7)–O(13)	2.862(7)
O(13)–O(14)	2.899(9)	O(12)–O(13)	2.959(8)
⟨O–O⟩	2.800	⟨O–O⟩	2.815
Ba(1) Polyhedron		Ba(2) Polyhedron	
O(1)–O(3)	2.886(8)	O(1)–O(2)	3.979(9)
O(1)–O(8)	3.443(7)	O(1)–O(3)	2.886(8)[a]
O(1)–O(11)	3.509(8)	O(1)–O(7)	3.171(7)
O(1)–O(14)	2.693(7)[a]	O(1)–O(11)	3.509(8)
O(2)–O(3)	4.080(8)	O(1)–O(12)	3.249(8)
O(2)–O(9)	3.623(7)	O(2)–O(4)	3.224(7)
O(2)–O(11)	3.583(8)	O(2)–O(11)	2.724(8)[a]
O(2)–O(14)	3.588(8)	O(2)–O(12)	3.092(8)
O(3)–O(11)	3.317(7)	O(3)–O(7)	3.600(7)
O(3)–O(11)	3.078(8)	O(3)–O(8)	3.607(8)
O(8)–O(9)	3.414(7)	O(3)–O(9)	3.289(8)
O(8)–O(11)	2.692(8)[a]	O(3)–O(11)	3.317(7)
O(8)–O(14)	3.704(8)	O(4)–O(9)	3.235(7)
O(9)–O(11)	3.923(8)	O(4)–O(10)	2.818(9)[a]
O(9)–O(11)	3.100(7)	O(4)–O(11)	3.690(8)
O(9)–O(14)	4.146(8)	O(4)–O(12)	4.502(8)
O(11)–O(11)	3.078(7)	O(7)–O(8)	3.016(7)
⟨O–O⟩	3.403	O(7)–O(10)	3.346(8)
		O(7)–O(12)	2.722(8)
		O(8)–O(9)	3.512(9)
		O(8)–O(10)	3.240(8)
		O(9)–O(11)	3.100(8)
		O(10)–O(12)	3.382(9)
		⟨O–O⟩	3.313
Ba(3) Polyhedron		Ba(4) Polyhedron	
O(1)–O(3)	2.886(8)[a]	O(2)–O(8)	2.713(8)[a]
O(1)–O(7)	3.171(7)	O(2)–O(10)	3.252(8)
O(1)–O(13)	2.804(8)[a]	O(2)–O(12)	3.092(7)
O(3)–O(7)	3.600(8)	O(2)–O(14)	3.588(8)
O(3)–O(10)	2.696(8)[a]	O(5)–O(6)	3.950(8)
O(3)–O(13)	4.672(9)	O(5)–O(7)	2.710(8)[a]
O(3)–O(14)	4.207(8)	O(5)–O(14)	3.457(7)
O(5)–O(6)	3.190(7)	O(5)–O(10)	3.447(7)
O(5)–O(10)	3.447(8)	O(5)–O(5′)	3.031(8)
O(5)–O(13)	3.586(8)	O(5′)–O(6)	3.178(7)
O(5)–O(14)	3.457(8)	O(5′)–O(12)	3.502(8)
O(6)–O(7)	3.516(7)	O(5′)–O(14)	3.529(9)
O(6)–O(13)	3.269(8)	O(6)–O(7)	3.213(8)
O(6)–O(14)	3.637(7)	O(6)–O(8)	3.993(8)
O(7)–O(13)	4.370(8)	O(6)–O(12)	3.753(8)
O(7)–O(14)	3.872(8)	O(7)–O(8)	3.016(7)
O(10)–O(13)	5.143(9)	O(7)–O(10)	3.346(8)
O(10)–O(14)	3.075(8)	O(8)–O(10)	3.373(8)
⟨O–O⟩	3.589	O(8)–O(12)	4.570(9)
		O(10)–O(14)	3.076(7)
		O(12)–O(14)	3.783(8)
		⟨O–O⟩	3.408

[a] Shared edge.

TABLE V

BOND ANGLES IN $Ba_2V_2O_7$

O(3)–V(1)–O(4)	111.3(3)°	O(2)–V(2)–O(4)	115.2(3)°
O(3)–V(1)–O(9)	111.5(3)	O(2)–V(2)–O(8)	108.0(3)[a]
O(3)–V(1)–O(10)	105.9(3)[a]	O(2)–V(2)–O(11)	106.8(3)
O(4)–V(1)–O(9)	109.8(3)	O(4)–V(2)–O(8)	111.6(3)[a]
O(4)–V(1)–O(10)	107.0(3)[a]	O(4)–V(2)–O(11)	108.8(3)
O(9)–V(1)–O(10)	111.3(3)	O(8)–V(2)–O(11)	106.0(3)[a]
⟨O–V(1)–O⟩	109.5	⟨O–V(2)–O⟩	109.4
O(1)–V(3)–O(6)	109.2(3)	O(5)–V(4)–O(7)	105.9(3)[a]
O(1)–V(3)–O(13)	106.7(3)[a]	O(5)–V(4)–O(12)	108.0(3)
O(1)–V(3)–O(14)	105.7(3)[a]	O(5)–V(4)–O(13)	111.2(3)
O(6)–V(3)–O(13)	111.7(3)	O(7)–V(4)–O(12)	107.8(3)[a]
O(6)–V(3)–O(14)	112.1(3)	O(7)–V(4)–O(13)	108.2(3)
O(13)–V(3)–O(14)	111.1(3)	O(12)–V(4)–O(13)	115.3(3)
⟨O–V(3)–O⟩	109.4	⟨O–V(4)–O⟩	109.4
V(1)–O(4)–V(2)	125.6(3)	V(3)–O(13)–V(4)	123.7(3)
O(1)–Ba(1)–O(3)	61.6(2)	O(1)–Ba(2)–O(2)	77.8(1)
O(1)–Ba(1)–O(8)	73.2(2)	O(1)–Ba(2)–O(3)	57.8(1)[a]
O(1)–Ba(1)–O(11)	80.7(2)	O(1)–Ba(2)–O(7)	64.6(1)
O(1)–Ba(1)–O(14)	58.1(2)[a]	O(1)–Ba(2)–O(11)	72.8(1)
O(2)–Ba(1)–O(3)	94.0(2)	O(1)–Ba(2)–O(12)	62.1(1)
O(2)–Ba(1)–O(9)	85.5(2)	O(2)–Ba(2)–O(4)	64.8(1)
O(2)–Ba(1)–O(11)	83.5(2)	O(2)–Ba(2)–O(11)	54.7(1)[a]
O(2)–Ba(1)–O(14)	81.6(2)	O(2)–Ba(2)–O(12)	59.0(1)
O(3)–Ba(1)–O(11)	72.9(2)	O(3)–Ba(2)–O(7)	82.5(2)
O(3)–Ba(1)–O(11)	81.3(2)	O(3)–Ba(2)–O(8)	79.2(2)
O(8)–Ba(1)–O(9)	73.5(2)	O(3)–Ba(2)–O(9)	73.2(2)
O(8)–Ba(1)–O(11)	55.9(2)[a]	O(3)–Ba(2)–O(11)	74.9(2)
O(8)–Ba(1)–O(14)	78.7(2)	O(4)–Ba(2)–O(9)	70.4(2)
O(9)–Ba(1)–O(11)	94.6(2)	O(4)–Ba(2)–O(10)	59.1(2)[a]
O(9)–Ba(1)–O(11)	70.8(2)	O(4)–Ba(2)–O(11)	83.5(2)
O(9)–Ba(1)–O(14)	98.7(2)	O(4)–Ba(2)–O(12)	78.1(2)
O(11)–Ba(1)–O(11)	69.8(2)	O(7)–Ba(2)–O(8)	64.8(2)
⟨O–Ba(1)–O⟩	77.3	O(7)–Ba(2)–O(10)	73.5(2)
		O(7)–Ba(2)–O(12)	55.1(1)[a]
		O(8)–Ba(2)–O(9)	76.3(2)
		O(8)–Ba(2)–O(10)	68.1(2)
		O(9)–Ba(2)–O(11)	68.9(2)
		O(10)–Ba(2)–O(12)	68.5(1)
		⟨O–Ba(2)–O⟩	69.1
O(1)–Ba(3)–O(3)	60.2(1)[a]	O(2)–Ba(4)–O(8)	55.9(1)[a]
O(1)–Ba(3)–O(7)	67.4(2)	O(2)–Ba(4)–O(10)	68.1(2)
O(1)–Ba(3)–O(13)	58.2(1)[a]	O(2)–Ba(4)–O(12)	66.8(2)
O(3)–Ba(3)–O(7)	79.8(2)	O(2)–Ba(4)–O(14)	79.2(2)
O(3)–Ba(3)–O(10)	55.9(2)[a]	O(5)–Ba(4)–O(6)	91.6(1)
O(3)–Ba(3)–O(13)	111.0(2)	O(5)–Ba(4)–O(7)	57.0(1)[a]
O(3)–Ba(3)–O(14)	96.9(2)	O(5)–Ba(4)–O(14)	75.7(1)
O(5)–Ba(3)–O(6)	72.6(2)	O(5)–Ba(4)–O(10)	72.8(2)
O(5)–Ba(3)–O(10)	75.5(2)	O(5)–Ba(4)–O(5′)	64.6(2)
O(5)–Ba(3)–O(13)	80.6(1)	O(5′)–Ba(4)–O(6)	70.4(2)

TABLE V—*continued*

O(5)–Ba(3)–O(14)	77.9(1)	O(5′)–Ba(4)–O(12)	77.1(2)
O(6)–O–Ba(3)–O(7)	80.0(2)	O(5′)–Ba(4)–O(14)	77.6(2)
O(6)–O–Ba(3)–O(13)	72.5(2)	O(6)–O–Ba(4)–O(7)	70.9(2)
O(6)–O–Ba(3)–O(14)	83.2(2)	O(6)–O–Ba(4)–O(8)	89.9(2)
O(7)–O–Ba(3)–O(13)	102.0(1)	O(6)–O–Ba(4)–O(12)	86.5(2)
O(7)–O–Ba(3)–O(14)	88.0(1)	O(7)–O–Ba(4)–O(8)	62.5(1)
O(10)–Ba(3)–O(13)	126.5(2)	O(7)–O–Ba(4)–O(10)	70.0(2)
O(10)–Ba(3)–O(14)	65.1(2)	O(8)–Ba(4)–O(10)	66.1(2)
⟨O–Ba(3)–O⟩	80.7	O(8)–Ba(4)–O(12)	105.2(2)
		O(10)–Ba(4)–O(14)	64.1(2)
		O(12)–Ba(4)–O(14)	85.0(2)
		⟨O–Ba(4)–O⟩	74.1

[a] Shared edge.

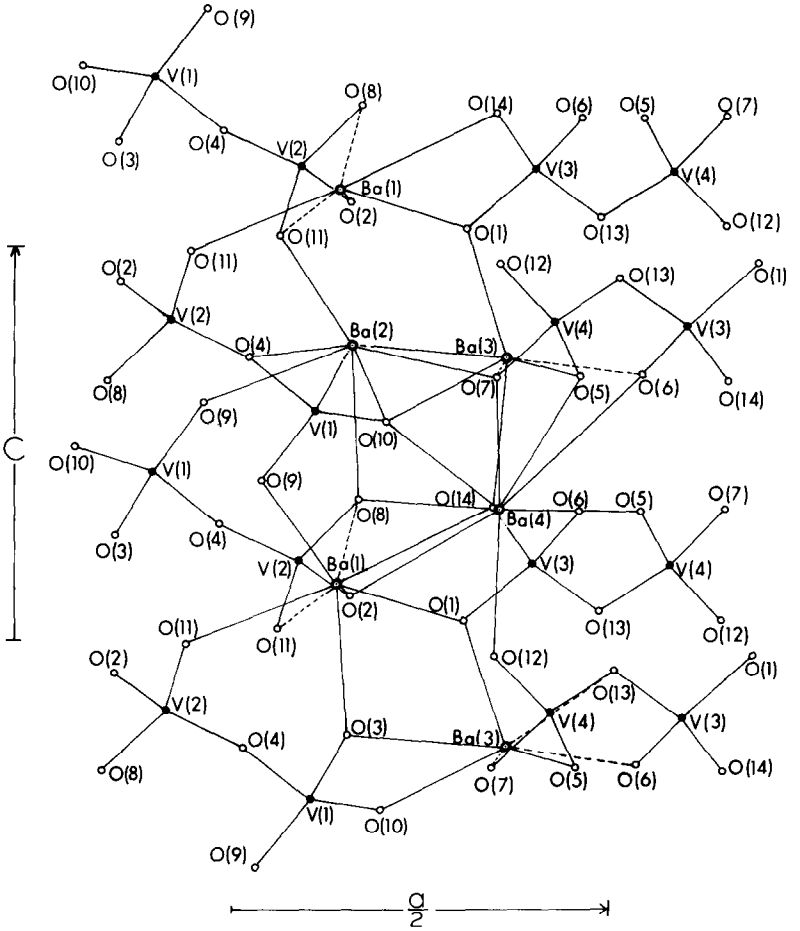

FIG. 1. An *ac* projection of the structure of $Ba_2V_2O_7$, showing the cation–oxygen bonds.

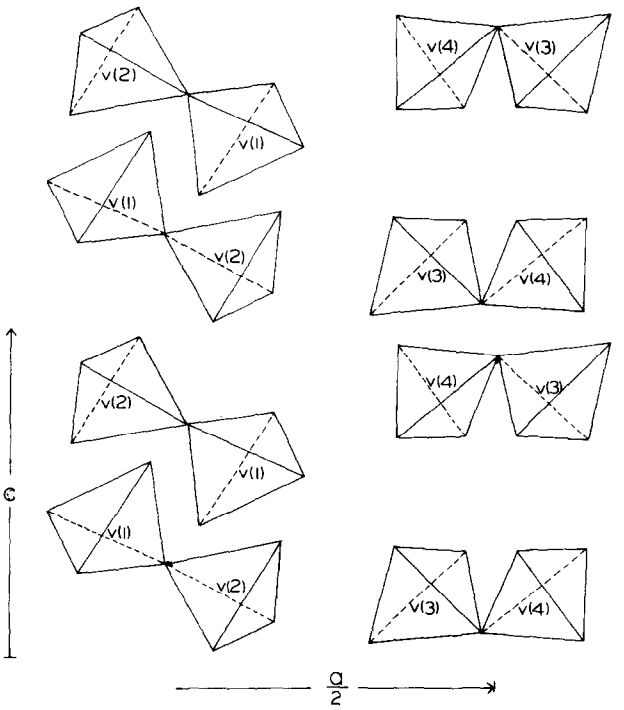

FIG. 2. An *ac* projection of the structure of $Ba_2V_2O_7$, showing the configurations of the divanadate groups. The typical dichromate-type sheets are seen here edge on.

TABLE VI

BOND STRENGTH[a] TABLE FOR $Ba_2V_2O_7$

	Ba(1)	Ba(2)	Ba(3)	Ba(4)	V(1)	V(2)	V(3)	V(4)	
O(1)	0.295	0.104	0.184				1.399		1.982
O(2)	0.338	0.107		0.236		1.353			2.034
O(3)	0.199	0.287	0.233		1.336				2.055
O(4)		0.228			0.927	0.914			2.069
O(5)			0.318	0.234 0.224				1.316	2.092
O(6)			0.336	0.336			1.446		2.118
O(7)		0.312	0.262	0.221				1.309	2.104
O(8)	0.145	0.190		0.170		1.446			1.951
O(9)	0.363	0.267			1.460				2.090
O(10)		0.207	0.187	0.161	1.357				1.912
O(11)	0.335 0.326	0.318				1.285			2.264
O(12)		0.117		0.254				1.433	1.804
O(13)			0.226				0.934	0.891	2.051
O(14)	0.244		0.256	0.246			1.301		2.047
	2.245	2.137	2.002	2.082	5.080	4.998	5.080	4.949	

[a] Bond strengths in valence units, calculated from the curves of Brown and Wu [10].

coordination number for the larger divalent (and monovalent) cations in crystals. However, a consideration of the bond strengths in $Ba_2V_2O_7$ allows unambiguous assignment of coordination numbers to all four Ba atoms. Table VI shows the bond strength table for $Ba_2V_2O_7$, calculated from the bond strength curves of Brown and Wu (*10*). All Ba–O distances less than 3.80 Å were included in the calculation, the maximum distance being Ba(2)–O(1) at 3.174 Å. The bond strength sums around Ba(3) and Ba(4) are reasonably close to the ideal value for cation coordination numbers of [8] and [9], respectively; in addition, the longest bonds from both cations are to oxygens that already show a slight deficiency with respect to ideal anion value, and hence these bonds cannot be ignored. The bond strength sums around Ba(1) and Ba(2) are considerably in excess of the ideal value for cation coordination numbers of [8] and [10], respectively. However, the longest bonds for both cations (Ba(1)–O(8) and Ba(2)–O(12)) are to anions that show bond strength sums of 1.951 and 1.804 v.u., respectively, both less than the ideal value of 2.0. Hence these interactions must be considered as significant to obtain a reasonable bond strength sum around the O(12) oxygen. Details of the Ba coordination are given in Fig. 3 and Tables III to V. Ba(1) is surrounded by eight oxygens between 2.655 and 3.026 Å, arranged in a distorted biaugmented triangular prism. Ba(2) is surrounded by ten oxygens between 2.706 and 3.174 Å, arranged in a distorted gyroelongated square dipyramid. Ba(3) is surrounded by eight oxygens between 2.705 and 2.926 Å, arranged in a distorted cubic antiprism. Ba (4) is surrounded by nine oxygens between 2.684 and 2.982 Å, arranged in a distorted tri-

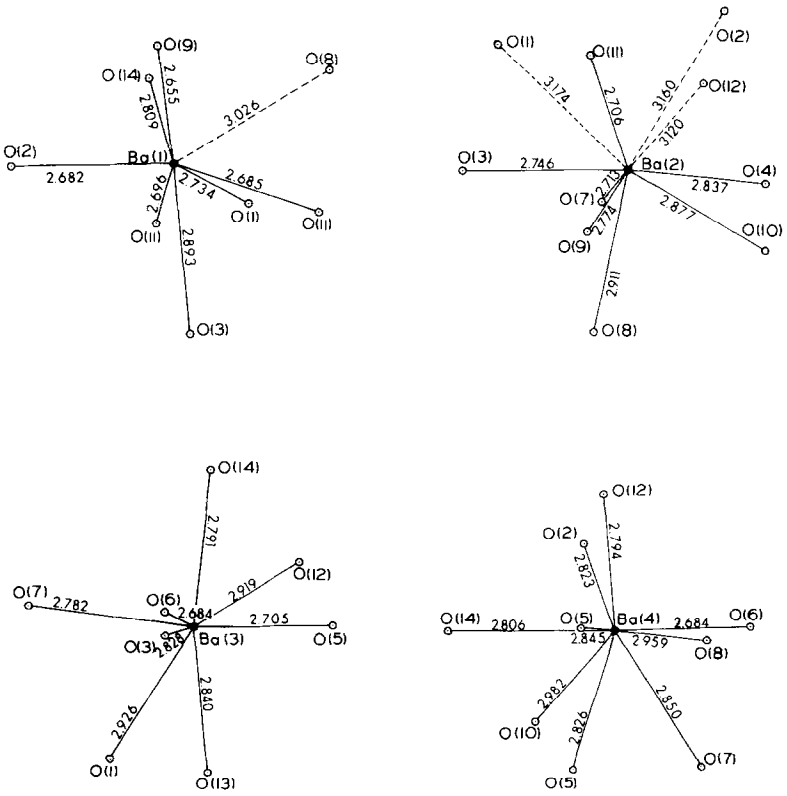

FIG. 3. Details of the Ba coordination in $Ba_2V_2O_7$.

TABLE VII

SELECTED DATA FOR DIVANADATE GROUPS

Structure	V–O(br)	V–O(nbr)	V–O–V	O(br)–C.N.	Configuration	Ref.
$Cd_2V_2O_7$	1.764(4)	1.702(13)	180	2	Staggered	(*11*)
$Mn_2V_2O_7$	1.759(6)	1.690(14)	180	2	Staggered	(*12*)
α-$Zn_2V_2O_7$	1.775(4)	1.697(4)	149.3(8)	2	Staggered	(*15*)
α-$Cu_2V_2O_7$	1.743(2)	1.698(3)	147.8(5)	2	Staggered	(*16*)
$Mg_2V_2O_7$	1.784(4)	1.696(2)	140.6(2)	3	Staggered	(*13*)
$K_2V_3O_8$	1.794(4)	1.675(4)	139.0(1)	3	Eclipsed	(*19*)
$Ca_2V_2O_7.2H_2O$	1.801(5)	1.689(3)	139	2	Eclipsed	(*18*)
β-$Cu_2V_2O_7$	1.770(4)	1.693(3)	138.2(1)	2	Staggered	(*17*)
$Ba_2V_2O_7$	1.821(4)	1.684(2)	125.6(3)	3	Eclipsed	—
	1.824(4)	1.685(2)	123.7(3)	3	Eclipsed	—
$Sr_2V_2O_7$	1.810(21)	1.688(11)	123	3	Eclipsed	(*2*)
	1.805(21)	1.703(11)	123	3	Eclipsed	(*2*)
$Pb_2V_2O_7$	1.817(8)	1.693(4)	122.1(6)	3	Eclipsed	(*14*)
$Co_2V_2O_7$	1.849(2)	1.694(1)	117.6(2)	3	Eclipsed	(*4*)
$Ni_2V_2O_7$	1.847(3)	1.692(2)	117.1(2)	3	Eclipsed	(*4*)

augmented triangular prism. There is a considerable variation in the ⟨Ba–O⟩ distances which vary from 2.77 to 2.90 Å. This results from the differences in the cation and anion coordination numbers in the different polyhedra. Using the ionic radii of Shannon (*1*), the following calculated (observed) distances are obtained for Ba(1), Ba(2), Ba(3), and Ba(4), respectively: 2.80(2.77), 2.89(2.90), 2.80(2.81), and 2.85(2.84) Å. This supports the cation coordination numbers assigned.

Table VII summarizes selected data for structures with divanadate groups. While there is considerable variation in ⟨V–O(br)⟩, from 1.743 Å in α-$Cu_2V_2O_7$ to 1.849 Å in $Co_2V_2O_7$, ⟨V–O(nbr)⟩ varies only from 1.675 Å in $K_2V_2O_8$ to 1.702 Å in $Cd_2V_2O_7$ with a mean value of 1.690 Å and rms deviation of 0.006 Å; in addition, there appears to be some tendency for divanadate groups in the staggered configuration to show slightly longer ⟨V–O(nbr)⟩ than those in the eclipsed configuration. Figure 4 shows the variation in ⟨V–O(br)⟩ with V–O(br)–V. There is a general tendency for longer ⟨V–O(br)⟩ distances to be associated with smaller V–O(br)–V angles. For V–O(br)–V angles less than 140°, the divanadate groups are in the eclipsed configuration, whereas for V–O(br)–V angles greater than 140°, the divanadate groups are in the staggered configuration. This change in configuration is generally accompanied by a change in the coordination number of the bridging anion of the divanadate group, with

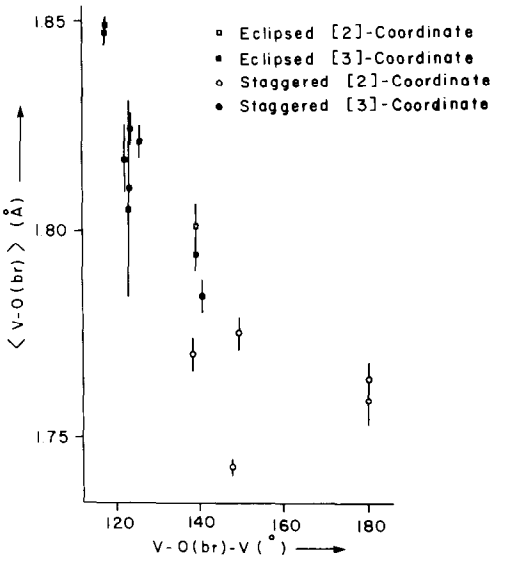

FIG. 4. The variation in ⟨V–O(br)⟩ with V–O(br)–V for structures containing divanadate groups.

the exception of those structures with V–O(br)–V ~ 140°. The change in the divanadate group configuration allows the bridging anion to bond to a nontetrahedral cation without the face-sharing that would probably be necessary if the divanadate group were in the staggered configuration. Thus cations with large coordination numbers, requiring more oxygens with which to bond, will generally require O(br) to be three-coordinate and hence be associated with divanadate groups in the eclipsed configuration. In addition, decrease of the V–O(br)–V angle promotes bonding between the bridging anion and the nontetrahedral cation. Thus smaller nontetrahedral cations should be accompanied by smaller V–O(br)–V angles, and Fig. 5 shows this to be the case. The gradual increase in ⟨V–O(br)⟩ as V–O(br)–V decreases should be accompanied by a concomitant increase in the strength of the bonding between O(br) and the nontetrahedral cation if the bond strength requirements of O(br) are to be satisfied; Fig. 6 shows the relationship between ⟨V–O(br)⟩ and the bond strength of the O(br)-nontetrahedral cation interaction, and indicates that this is the case for the structures where O(br) is [3]-coordinate. However, for the structures where O(br) is [2]-coordinate, ⟨V–O(br)⟩ varies between 1.743(2) Å for α-$Cu_2V_2O_7$ and 1.801(5) Å for $Ca_2V_2O_7 \cdot 2H_2O$, and a bond strength model cannot adequately account for this variation.

Baur (*20*) has shown that cation–oxygen bond lengths may be related to Δp_0, the difference between the formal Pauling bond strength and the mean bond strength in the specific coordination polyhedron by the equation $d_{T-O} = a + b\Delta p_0$, and Gopal (*21*) has derived the constants for this equation relating to tetrahedral vanadates. Figure 7 compares this curve to the divanadate structures discussed here. Although the overall fit is fairly good (rms deviation = 0.018 Å), there are individual deviations of up to 0.061 Å (for α-$Cu_2V_2O_7$). In general, much of the deviation can be a consequence of the distorted nature of the *M*–O polyhedra (*14*). However, this does not account for the large deviations exhibited by the V–O(br) bonds of the staggered divanadate groups. Brown and Shannon (*22*) have suggested that high bond strength sums (short ⟨T–O(br)⟩ distances) in a series of

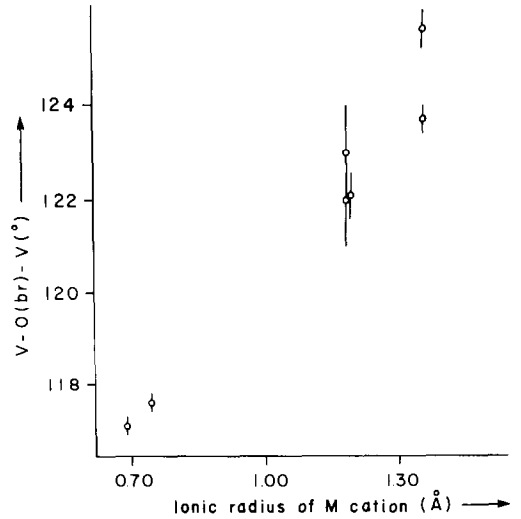

FIG. 5. The variation in V–O(br)–V with nontetrahedral cation radius (for [6]-fold coordination) for the dichromate-like divanadates.

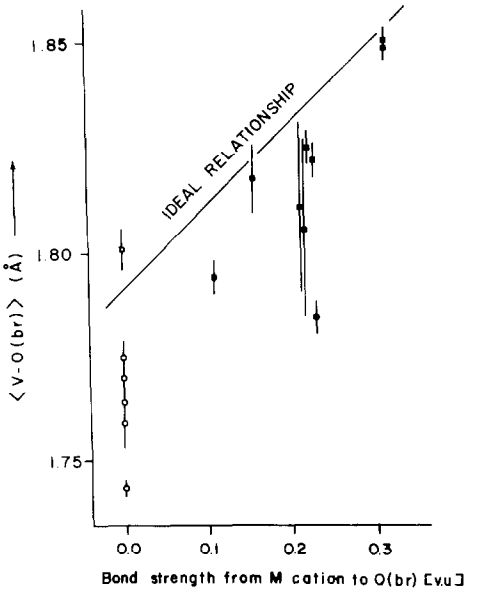

FIG. 6. The variation in ⟨V–O(br)⟩ with the bond strength of the O(br)–M cation bond. Legend as for Fig. 4.

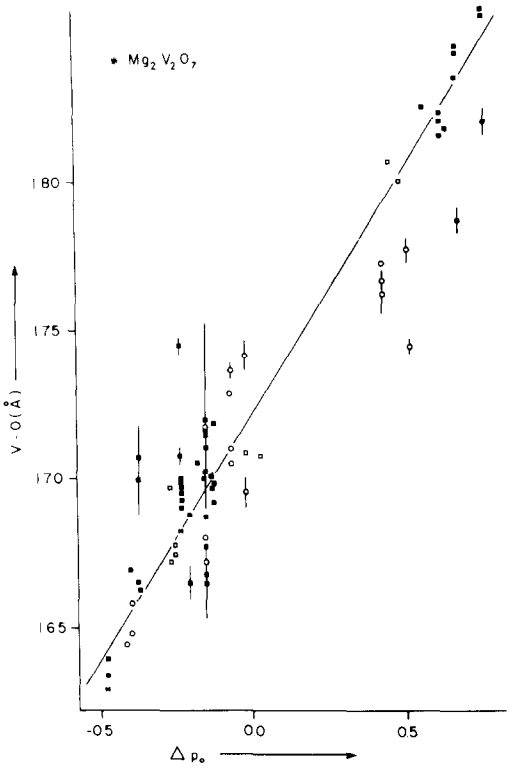

FIG. 7. The variation in V–O as a function of Δp_0 (see text). The solid line is the relationship derived by Gopal (*21*) for tetrahedral V^{+5}–O bonds.

pyrophosphates are indicative of anomalously large thermal motion. Although this may have some effect in the thortveitite isotypes, it is unlikely that this can account for such deviations as that shown by α-$Cu_2V_2O_7$.

From the discussion given above, it is apparent that although some of the variations in the divanadate group configuration can be rationalized using a bond strength model, the variation in the bridging V–O bond lengths in the thortveitite-like compounds cannot. As the bond strength requirements of the bridging oxygen appear to be a key factor in these structures, this problem must be resolved before the reasons for the wide variety of structure types in this series are understood.

Acknowledgments

Financial support for this study was provided by the National Research Council of Canada (grants to C. Calvo and R. B. Ferguson) and the University of Manitoba.

References

1. R. D. SHANNON, *Acta Crystallogr.* A **32**, 751 (1976).
2. J. A. BAGLIO AND J. N. DANN, *J. Solid State Chem.* **4**, 87 (1972).
3. I. D. BROWN AND C. CALVO, *J. Solid State Chem.* **1**, 173 (1970).
4. E. E. SAUERBREI, R. FAGGIANI, AND C. CALVO, *Acta Crystallogr. B* **30**, 2907 (1974).
5. R. KOHLMULLER AND J. PERRAUD, *Bull. Soc. Chim. Fr.* **1964**, 642 (1964).
6. A. A. FORTIEV, V. V. MAKAROV, V. L. VOLKOV, AND L. L. SURAT, *Russ. J. Inorg. Chem.* **14**, 144 (1969).
7. J. M. STEWART, Univ. of Maryland; adapted to the CDC 6400 computer by H. D. Grundy, McMaster Univ.
8. D. T. CROMER AND J. B. MANN, *Acta Crystallogr.* **24**, 321 (1968).
9. D. T. CROMER AND D. LIBERMAN, *J. Chem. Phys.* **53**, 1891 (1970).
10. I. D. BROWN AND K. K. WU, *Acta Crystallogr. B* **32**, 1957 (1976).
11. P. K. L. AU AND C. CALVO, *Canad. J. Chem.* **45**, 2297 (1967).
12. E. DORM AND B. MARINDER, *Acta Chem. Scand.* **21**, 590 (1967).
13. R. GOPAL AND C. CALVO, *Acta Crystallogr. B* **30**, 2491 (1974).
14. R. D. SHANNON AND C. CALVO, *Canad. J. Chem.* **51**, 70 (1973).
15. R. GOPAL AND C. CALVO, *Canad. J. Chem.* **51**, 1004 (1973).
16. C. CALVO AND R. FAGGIANI, *Acta Crystallogr. B* **31**, 603 (1975).
17. D. MERCURIO-LAVAUD AND B. FRIT, *C.R. Acad. Sci. Paris, Ser. C.* **277**, 1101 (1973).
18. J. A. KONNERT AND H. T. EVANS, JR. *Acta Crystallogr. B* **31**, 2688 (1975).
19. J. GALY AND A. CARPY, *Acta Crystallogr. B* **31**, 1794 (1975).
20. W. H. BAUR, *Trans. Amer. Cryst. Assoc.* **6**, 129 (1970).
21. R. GOPAL, Ph.D. Thesis, McMaster Univ., Hamilton, Ontario, 1972.
22. I. D. BROWN AND R. D. SHANNON, *Acta Crystallogr. A* **29**, 266 (1973).
23. E. A. KUZ'MIN, V. V. ILYUKHIN, AND N. V. BELOV, *Dokl. Akad. Nauk SSSR* **173**, 1078 (1967).
24. J. K. BRANDON AND I. D. BROWN, *Canad. J. Chem.* **46**, 933 (1968).